









## An empirical investigation and computational modeling of volatile organic compound (VOCs) elimination from aqueous solutions by means of Pervaporation



Salam H. Rasheed<sup>a</sup>, Salah S. Ibrahim<sup>a</sup> , Asmaa F. Abbas<sup>a</sup> , Raed A. Al-Jaboori<sup>\*b</sup> , Zeinab Abbas Jawad<sup>c</sup> , Low Siew Chun<sup>d</sup> , Qusay F. Alsahy<sup>a</sup> 

<sup>a</sup> Chemical Engineering Dept., University of Technology-Iraq, Alsina'a street, 10066 Baghdad, Iraq.

<sup>b</sup> NYUAD Water Research Centre, New York University Abu Dhabi Campus, Abu Dhabi P.O. Box 129188, United Arab Emirates.

<sup>c</sup> Chemical Engineering Dept., College of Engineering, University of Qatar, Doha, Qatar.

<sup>d</sup> School of Chemical Engineering, Universiti Sains Malaysia (USM)14300 Nibong Tebal, Penang, Malaysia.

\*Corresponding author Email: [raa9914@nyu.edu](mailto:raa9914@nyu.edu)

### HIGHLIGHTS

- This study separated benzene and toluene using a PDMSTM4060 membrane.
- The UNIQUAC and conventional driving force models adequately predicted VOC and water permeation.
- VOC temperature and activity were important elements in the diffusivity correlations.

### ABSTRACT

The present study harnessed a commercially available polydimethylsiloxane (PDMSTM4060) membrane designed for the selective separation of soluble benzene (C<sub>6</sub>H<sub>6</sub>) and toluene (C<sub>7</sub>H<sub>8</sub>) compounds from an aqueous solution employing pervaporation (PV). Two distinct mathematical models, namely the universal quasi-chemical (UNIQUAC) model and the conventional driving force model, were formulated to replicate the intricate transport mechanisms of both organic solvent and water across these membranes. These models were instrumental in projecting the membrane's performance across diverse operational scenarios. The anticipated results were rigorously compared with experimental data to validate the projected outcomes for non-ideal volatile organic compounds (VOCs)-water systems within the membrane. Correlations pertaining to diffusivity were derived from the model and experimental pervaporation data. Utilizing the UNIQUAC theory and derived diffusivity correlations enabled the estimation of VOCs and water permeation through the commercial membrane. Notably, for the PDMSTM4060 membrane, the established diffusivity correlations for VOCs and water were contingent upon temperature variations and the activity of VOCs. The anticipated permeation flux of VOCs and water through the membranes was prognosticated using the mass transport model in conjunction with the established diffusivity correlations. The resultant findings showcased a robust concurrence between the predictive model and the empirical data, affirming the reliability of the proposed approach.

### ARTICLE INFO

**Handling editor:** Mustafa H. Al-Furaiji

#### Keywords:

Pervaporation  
PDMS  
Benzene  
Toluene  
UNIQUAC model

## 1. Introduction

The interest in drinking water is expanding quickly since the world's population is estimated to increase by another 40–50% by 2050. Besides preserving the environment from pollution by volatile organic compounds (VOCs) and protecting river water and aquatic life, these materials must be disposed of using modern, more effective, less costly methods. Many industrial applications use organic solvents in their technological processes to have products such as refrigerants, plastics, adhesives, paints, and petroleum products [1]. Pervaporation constitutes a separation technique wherein a semi-permeable membrane is employed to selectively extract components, predominantly volatile substances, from a liquid mixture. Within pervaporation, a liquid feed mixture interfaces with one facet of the membrane, while the resultant permeate emerges as vapor from the opposing side. The membrane's characteristics may vary, exhibiting either hydrophobic or hydrophilic traits contingent upon the intended application [2]. The facilitation of transport across the membrane is instigated by the discrepancy in partial vapor pressure between the initial feed solution and the emerging permeate vapor. Diverse methodologies sustain this vapor pressure differential.

Conventionally, a vacuum pump is employed at the laboratory scale to uphold vacuum conditions on the permeate side. In contrast, in industrial settings, the most cost-effective approach involves the spontaneous cooling and subsequent condensation of the permeate vapor, generating a partial vacuum [3].

Comprehending the intricacies of mass transfer mechanisms within the pervaporation (PV) process is a pivotal factor in selecting suitable membranes and refining membrane designs to achieve heightened flux rates and superior separation factors. The development of a comprehensive mathematical model governing mass transfer assumes paramount importance, expediting laboratory experimentation timelines, facilitating improved membrane material design, and addressing potential issues encountered during the PV process [4]. The industrial application of the PV process necessitates formulating a mathematical framework delineating mass transfer phenomena. This mathematical model focuses on elucidating the intricacies of mass transfer within the membrane's active layer, where compound transport induces a phase transition. Multiple process variables wield significant influence over the PV separation process, encompassing operational parameters such as feed temperature, concentration, permeate pressure, and feed flow rate. Additionally, the inherent properties of the membrane itself—be it hydrophilic or hydrophobic—alongside factors like the physical structure of the membrane surface, degree of membrane cross-linking, and extent of swelling profoundly dictate the mechanism of mass transport [5].

Numerous models have emerged to delineate the pervaporation process, classified into empirical, theoretical, and semiempirical categories [6, 7]. Abrams and Prausnitz pioneered the UNIQUAC model 1975, initially crafted to prognosticate the equilibrium within liquid-liquid and liquid-vapor states across binary and multi-component systems encompassing polymers [8]. The inception of the UNIFAC theory amalgamated the UNIQUAC model with Wilson's concept from 1962, conceptualizing a liquid mixture constituted by functional groups within a solution [9, 10]. Subsequent enhancements to the UNIFAC theory ensued with incorporating a free volume contribution term, as elucidated by Oishi and Prausnitz in 1978, wherein satisfactory agreements were observed across 13 binary solvent-polymer systems [11]. Expanding upon this groundwork, Goydan et al. (1989) extended the Oishi and Prausnitz UNIFAC model, extending its predictive capacity to encompass the sorption behavior of various organic compounds like alcohols and acids within diverse polymers, demonstrating acceptable alignment with empirical data [12]. Further advancements were made by Heintz and Stephan in 1992 and 1994, employing the UNIQUAC model to anticipate the sorption tendencies of non-ideal systems characterized by a dense selective layer, exemplified in scenarios such as alcohol-water mixtures within PVA [13, 14].

This investigation employed a mathematical framework to elucidate the exponential reliance of the diffusion coefficient on the activity of volatile organic compounds (VOCs) within a hydrophobic commercial membrane (PDMSTM4060) and its plasticization parameter. The plasticization parameter, influenced by feed temperature and VOC concentration, significantly affects this coefficient. The construction of a mass transfer model to predict VOCs and water mass transfer through the selective separating layer using diffusivity correlations as a fundamental basis was undertaken in this study. Within this context, the UNIQUAC model was employed to simulate sorption equilibria for nonideal mixtures of VOCs and water in hydrophobic membranes. The diffusion coefficient for VOCs and water traversing PDMS membranes was estimated by utilizing the solution-diffusion mass transport model alongside experimental data obtained from the pervaporation process [15].

## 2. Theory

Two approaches exist to elucidate the transport of mass across a membrane in the pervaporation process: (i) the solution diffusion model and (ii) the pore flow model [16, 17].

### 2.1 Preferential sorption-capillary flow (PSCF) mechanism

Initially introduced by Sourirajan et al. in 1987, the pore flow mechanism, extensively expounded upon by subsequent researchers such as Okada et al. [18-20], delineates the mass transport process within porous pervaporation membranes. This mechanism relies on the porous nature of the membrane, where the targeted substance traverses from upstream to downstream through minute capillary channels and subsequently evaporates downstream due to the exertion of vacuum pressure [21, 22]. Consequently, the pervaporation (PV) process is perceived as a sequential amalgamation of liquid and vapor transport [23, 24]. The efficacy of this mechanism is contingent upon factors like pore size and distribution within the membrane, the molecular dimensions of the target substance, and the interplay between the membrane and the said substance. The pore flow model comprises three distinct stages: (i) liquid movement from upstream to the pore until the liquid-vapor phase boundary (Z1); (ii) the transition from liquid to vapor at the interface boundary between liquid and vapor phases; and (iii) the vapor transfer from the interphase boundary to the pore outlet (Zv) [25].

As depicted in Figure (1A), the pore-flow model assumes uniform concentrations of solvent and solute within the membrane, where the chemical potential gradient across the membrane is primarily expressed as a pressure gradient [20]. The separation process occurs as one of the permeants is excluded or filtered from specific membrane pores through which other permeants pass. According to the pore flow model, a phase transition occurs within the membrane when the pressure of the permeate vapor falls below the saturated vapor pressure of the initial feed liquid [26]. In Figure (1B) the chemical potential and the pressure change across the membrane while the activity remains constant [27]. Nonetheless, the pore-flow model may overlook the interaction between membrane materials and the penetrating substances, rendering it less suitable for membranes significantly affected by swelling due to the feed liquid solution [25].

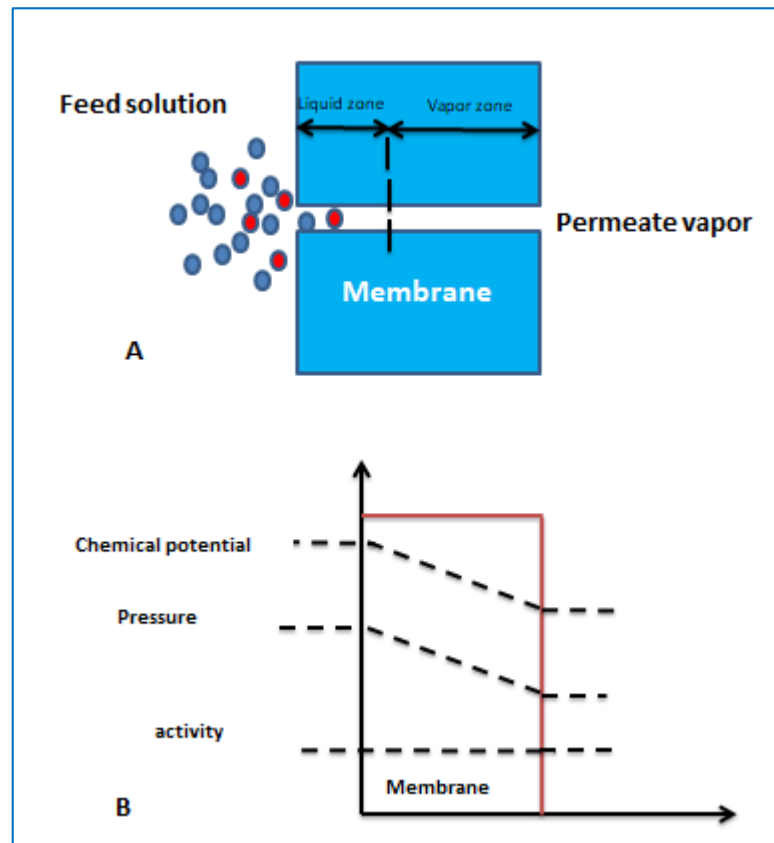


**Figure 1:** (A) Schema of mass transfer in the pore-flow model; (B) chemical potential, pressure, and activity gradients in the pore-flow model

The total flux in the pore flow model can be calculated as in the following [19]:

$$J_i = \left[ \frac{Q}{L} (P_f - P_{\text{sat,mix}}) + \frac{B_i}{L} (P_{i,\text{sat}}^2 - P_{i,p}^2) + \frac{B_j}{L} (P_{i,\text{sat}}^2 - P_{j,p}^2) \right] (y_i M_i + y_j M_j) \quad (1)$$

where  $P_{i,p}$  and  $P_{i,\text{sat}}$  are partial pressures of component  $i$  on permeate and feed sides,  $P_f$  is liquid feed pressure at pore inlet,  $L$  is membrane thickness,  $y_i$  and  $M_i$  are the permeate mole fraction and molecular weight of component  $i$ , respectively.  $Q$ ,  $B_i$ ,  $B_j$  are constants. It is apparent from Equation (1) that the total permeation flux depends on the pressure gradient across the membrane.

## 2.2 Solution-diffusion model

The solution-diffusion mechanism is one of the predominant models extensively employed to elucidate matter transference through a dense membrane within the pervaporation process [28, 29]. Originating in 1866, Graham was the first to propose this mechanism to explain gas permeability through a rubber barrier, subsequently gaining traction among researchers in the pervaporation (PV) realm due to its compatibility with empirical experimentation [30].

Pervaporation processes utilize non-porous membranes hinging on the solution diffusion mechanism, comprising three primary phases. Initially, sorption involves the adherence of the target substance to the membrane surface. Subsequent diffusion through the membrane is contingent upon the molecular affinity between the material and the membrane, facilitating penetration through polymeric chains. Finally, desorption ensues, transitioning the material phase from liquid to vapor owing to downstream vacuum pressure [7, 27]. Typically, the last phase is omitted in model computations owing to its rapid occurrence facilitated by downstream vacuum pressure [31, 32]. As illustrated in Figure (2A), the model considers these sequential phases wherein permeate materials segregate due to differential solubility within the membrane and subsequent diffusion across it [33-35]. In Figure (2B) the chemical potential and the activity change across the membrane while the pressure remains constant [27]. The solution-diffusion model assumes uniform pressure within the membrane, expressing the chemical potential gradient solely as a concentration gradient across the membrane [34].

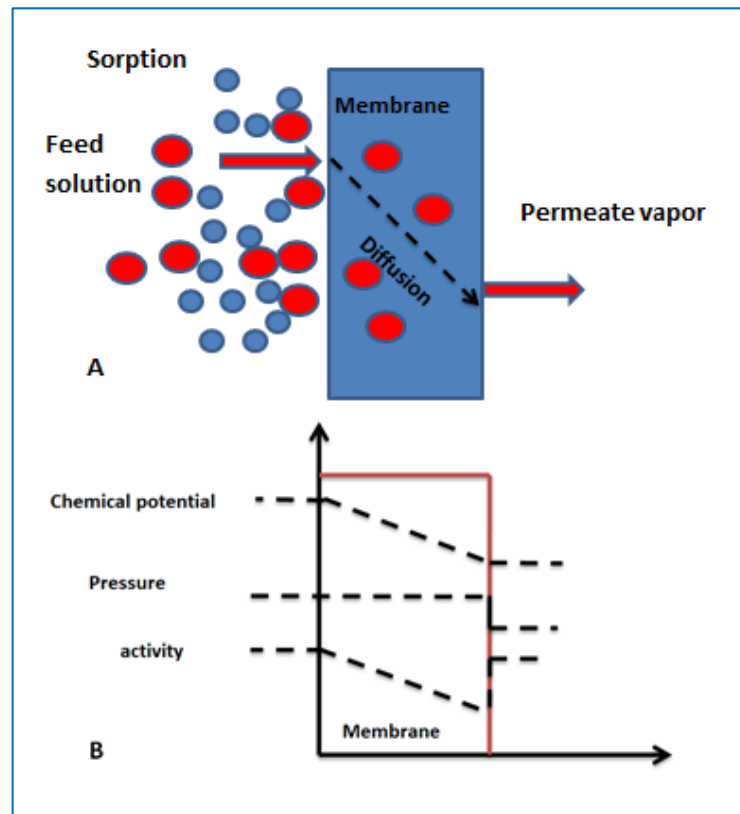


**Figure 2:** (A) Schema of mass transfer in solution-diffusion model; (B) chemical potential, pressure, and activity gradients in solution-diffusion model

Based on the solution-diffusion mechanism, the transport equation can be derived as follows [27, 28]:

$$J_i = -L_i \frac{d\mu_i}{dz} \quad (2)$$

where ( $J$ ) is the permeation rate of component ( $i$ ) through a membrane, ( $d\mu_i/dz$ ) is the chemical potential gradient across the membrane, and  $L_i$  is a proportionality coefficient.

Under isothermal conditions (constant temperature), the chemical potential ( $\mu_i$ ) in concentration and pressure-driven processes is:

$$\mu_i = \mu_i^0 + RT \ln(C_i) + v_i(p - p_i^0) \quad (3)$$

The chemical potential gradient ( $d\mu_i$ ) is given as:

$$d\mu_i = RT d \ln(C_i) + V_i dp \quad (4)$$

where  $\mu_i^0$  is the electrochemical potential,  $T$  is the temperature,  $R$  is the gas constant,  $C_i$  is the molar concentration of component  $i$ , and  $V_i$  is the molar volume. As mentioned before, the pressure within the membrane is assumed to be constant ( $dp = 0$ ), therefore combining Equations (2) and (4) gives:

$$J_i = -\frac{RTL_i}{C_i} \frac{dC_i}{dz} \quad (5)$$

Replace  $RTL_i/c_i$  by diffusion coefficient  $D_i$ , and integrating the Equation (5) across the membrane provides:

$$J_i = -D_i \frac{(C_{i(s)}^f - C_{i(s)}^p)}{l} \quad (6)$$

where  $L$  is the membrane thickness,  $C_{i(s)}$  is the concentration of component ( $i$ ) in the membrane, and the superscript  $f$  and  $p$  represent the feed and permeate side, respectively.

The concentration at the membrane interface can be obtained by Henry's law:

$$C_{i(s)}^f = K_i P_i^f \quad (7)$$

$$C_{i(s)}^p = K_i P_i^p \quad (8)$$

where  $K_i$  is the solubility or adsorption coefficient,  $p_i^f$ ,  $p_i^p$  are the vapor pressure on the feed side and permeate side, respectively. Thus,

$$J_i = -D_i K_i \frac{(p_i^f - p_i^p)}{l} \quad (9)$$

Based on the solution-diffusion model, the permeability coefficient  $P_i$  is given by the product of the diffusivity  $D_i$  and the solubility coefficient  $K_i$  ( $P_i = D_i K_i$ ). Thus,

$$J_i = -P_i \frac{(p_i^f - p_i^p)}{l} \quad (10)$$

The measure of substance absorbed by a membrane at equilibrium delineates a thermodynamic attribute known as solubility, a characteristic reliant upon the molecular composition of permeating molecules and the membrane material itself. Conversely, diffusivity serves as a kinetic parameter denoting the rate of penetrant movement across the membrane, influenced by the membrane's microstructure morphology, the permeating molecules' dimensions and configuration, and the reciprocal interactions between the membrane material and the penetrating molecules [36].

Within the ambit of the solution-diffusion model, investigation entails scrutinizing the sorption of various compounds into the membrane followed by their subsequent diffusion across it. Numerous scholars have undertaken theoretical explorations into the sorption and diffusion of liquid permeation through dense membranes within the framework of the solution-diffusion model [37, 38].

### 2.3 Calculation of the activity of VOCs

According to the UNIQUAC theory, a component  $i$ 's ( $a_i$ ) activity in a multi-component system is divided into two parts: (i) a combinatorial portion ( $a_i^C$ ) caused by variations in molecular size and shape, which contribute to the entropy of mixing, and (ii) a residual portion ( $a_i^R$ ) caused by energetic interactions/enthalpy of mixing. Consequently, the following formula can be used to express the activity of component  $i$  ( $a_i$ ) in a multi-component liquid combination:

As per the UNIQUAC theory, the activity ( $a_i$ ) of a specific component  $i$  within a multi-component system is partitioned into two distinct segments: (i) a combinatorial component ( $a_i^C$ ) attributable to discrepancies in molecular dimensions and configuration, thus influencing the entropy of mixing, and (ii) a residual component ( $a_i^R$ ) arising from energetic interactions or the enthalpy of mixing [39]. Consequently, the ensuing formula encapsulates the expression of the activity of component  $i$  ( $a_i$ ) within a multi-component liquid amalgamation:

$$\ln a_i = \ln a_i^C + \ln a_i^R \quad (11)$$

$$\ln a_i(x_1, \dots, x_n) = \ln \Phi_i + \frac{z}{2} q_i \ln \left[ \frac{\theta_i}{\Phi_i} \right] + l_i - \sum_{j=1}^n \Phi_j \frac{r_j}{r_i} l_j - q_i^* \ln \sum_{j=1}^n \theta_j^* \tau_{ji} + q_i^* - q_i^* \sum_{k=1}^n \frac{\theta_k^* \tau_{kj}}{\sum_{k=1}^n \theta_k^* \tau_{kj}} \quad (12)$$

where,

$$\Phi_i = \frac{r_i x_i}{\sum_{j=1}^n r_j x_j} \quad (13)$$

$$\theta_i = \frac{q_i x_i}{\sum_{j=1}^n q_j x_j} = \frac{\left[ \frac{q_i \Phi_i}{r_i} \right]}{\sum_{j=1}^n \left[ \frac{q_j \Phi_j}{r_j} \right]} \quad (14)$$

$$\theta_i^* = \frac{q_i^* x_i}{\sum_{j=1}^n q_j^* x_j} = \frac{\left[ \frac{q_i^* \Phi_i}{r_i} \right]}{\sum_{j=1}^n \left[ \frac{q_j^* \Phi_j}{r_j} \right]} \quad (15)$$

$$l_i = \frac{z}{2} (r_i - q_i) - (r_i - 1) \quad (16)$$

In this context,  $n$  represents the count of constituents within the blend, while  $x_i$  pertains to the mole fraction of a particular component. Furthermore,  $\theta$  and  $\theta^*$  correspond to the surface fractions specific to the component, and  $\Phi_i$  denotes the volume fraction attributed to the said component. Parameters denoted by  $Z$ ,  $r$ ,  $l$ ,  $q$ , and  $q^*$  relate intricately to the geometric properties of the molecules involved, encompassing both the shape and size. The binary intermolecular interaction parameters,  $\tau_{ij}$  and  $\tau_{ji}$ , are ascertainable by fitting the liquid mixture's vapor-liquid equilibrium (VLE) data to the aforementioned equation. Within polymeric systems, due to the notably minute polymer mole fraction relative to other solvent types, it proves more convenient to articulate  $a_i$  as a function of the component's volume fraction. Thus, the thermodynamic activity of component  $i$  ( $a_i$ ) within a multi-component liquid blend existing within the membrane in the polymeric system is articulated as follows:

$$\ln a_i(\Phi_1, \dots, \Phi_i, \dots, \Phi_n, \Phi_p) = \ln \Phi_i + \frac{z}{2} q_i \ln \left[ \frac{\theta_i}{\Phi_i} \right] + l_i - \sum_{j=1}^n \Phi_j \frac{r_i}{r_j} l_j - r_i \Phi_p \left[ \frac{z}{2} \left[ 1 - \frac{q_p}{r_p} \right] - 1 \right] - q_i^* \ln \sum_{j=1}^n \theta_j^* \tau_{ji} + q_i^* - q_i^* \sum_{j=1}^n \frac{\theta_j^* \tau_{ij}}{\sum_{k=1}^n \theta_k^* \tau_{kj}} \quad (17)$$

Equation (17) can be utilized to appropriately fit the vapor sorption data of a pure component, enabling the derivation of the binary interaction parameter  $\tau_{ip}$ . In Equations (12) and (17), supplementary terms involving  $q^*$  and  $\theta^*$  were integrated to accommodate the hydrogen bonding prevailing within the system. When employing a PVA membrane, Heintz and Stephan (1994) effectively employed the UNIQUAC model to anticipate the sorption behavior of alcohols sourced from aqueous solutions [13]. Nevertheless, a notable limitation of this model is the difficulty in acquiring requisite information for computing the values of the binary interaction parameters, thereby impeding its practical application.

## 2.4 Diffusion

The second phase within the solution-diffusion model pertains to diffusion, constituting a stage governed by rates in the pervaporation process. It involves the migration of distinct species contingent upon the variance in chemical potential through dense polymeric membranes. Several factors, encompassing interactions between diffusing constituents, polymer architecture, size of the permeating compound, and the extent of membrane swelling, significantly influence the diffusion coefficient. The concentrations of permeating elements within the polymer structure play a pivotal role in determining the membrane's swelling extent. As the membrane swells, the free volume amid polymer chains expands, augmenting the diffusivity of penetrating materials and consequently enhancing the mass transfer rate [31].

Separating organic compounds (like benzene or toluene) from water engenders a non-ideal ternary system characterized by robust hydrogen bonding and plasticizing effects. To enhance the precision of forecasting such separations employing PDMS membranes, the proposed model amalgamates Equations (2) and (17) – the UNIQUAC group contribution model for predicting membrane sorption equilibrium in non-ideal systems.

Given the scarcity of diffusivity correlations elucidating the passage of organic component-water mixtures through PDMS membranes, empirical diffusivity correlations were derived from pervaporation experiment data based on organic feed concentration and feed temperature. These correlations were employed to predict membrane separation performance. An underlying assumption posits constant diffusion coefficients across the polymeric membrane for each organic content and feed temperature. To aptly foresee the separation of an organic component from water using PDMS membranes, the model fuses the core mass transport equation with the UNIQUAC group-contribution equation. An innovative facet of this model lies in its novel postulate that the diffusion coefficients within the polymer hinge not only on the organic concentration in the feed but also on the feed temperature.

The following represents the continuity equation illustrating the passage of component  $i$  across the membrane:

$$\rho_i \left( \frac{d\Phi_i}{dt} + u \nabla \Phi_i \right) = \nabla (-J_i) + R_a \quad (18)$$

where  $\rho$  is density,  $u$  is the fluid velocity (m/s),  $J_i$  is the flux of mass transfer,  $t$  is the time in seconds (s),  $\Phi_i$  is the component volume fraction, and  $R_a$  is the rate of reaction (mol/m<sup>3</sup>.s).

Diffusion is the main factor in mass movement inside the membrane, whereas convective mass transfer is barely noticeable. Hence, the continuity equation for the transport of component  $i$  through the membrane at steady-state can be expressed as follows:

$$\nabla (-J_i) = 0 \quad (19)$$

The following form can be used to represent Equation (2) for hydrophobic polymeric membranes:

$$J_i = -C_i L_i \frac{d\mu_i}{dz} \quad (20)$$

From the following equation, the chemical potential can be calculated.

$$\mu_i = \mu_i^0 + RT \ln a_i + V_i P \quad (21)$$

From Equation (21), the derivative of chemical potential can be obtained as:

$$d\mu_i = RT \, d\ln a_i + V_i dP \quad (22)$$

where  $P$  is the system's pressure,  $a_i$  is the activity of component  $i$ , and  $V_i$  is the molar volume. The pressure across the membrane is constant in the solution-diffusion model of the pervaporation process. Thus, the Equation (22) is expressed as follows:

$$d\mu_i = RT \, d\ln a_i \quad (23)$$

By connecting Equation (23) and (20), the permeation flux is calculated as follows:

$$J_i = -C_i L_i RT \frac{d\ln a_i}{dz} \quad (24)$$

The thermodynamic diffusivity of component  $i$  ( $D_{iT}$ ) through the polymer can be expressed as:

$$D_{iT} = L_i RT \quad (25)$$

where  $C_i$  is the concentration of component  $i$  that is related to the volume fraction according to the following relation:

$$C_i = \rho_i \Phi_i \quad (26)$$

Therefore, Equation (24) can be rewritten as:

$$J_i = -D_{iT} \Phi_i \rho_i \frac{d\ln a_i}{dz} \quad (27)$$

When the coupling of fluxes is considered in the ternary system consisting of binary solvents and the membrane, the volume fraction of all components  $i$  and  $j$  in the polymeric membrane will affect the activity of component ( $a_i$ ). Thus, the expression (27) can be expressed as follows:

$$J_i = -D_{iT} \Phi_i \rho_i \left[ \frac{d\ln a_i}{d\Phi_i} \cdot \frac{d\Phi_i}{dz} + \frac{d\ln a_i}{d\Phi_j} \cdot \frac{d\Phi_j}{dz} \right] \quad (28)$$

$$J_j = -D_{jT} \Phi_j \rho_j \left[ \frac{d\ln a_j}{d\Phi_i} \cdot \frac{d\Phi_i}{dz} + \frac{d\ln a_j}{d\Phi_j} \cdot \frac{d\Phi_j}{dz} \right] \quad (29)$$

The permeation flow of component  $i$  depends on both its concentration gradient and the concentration gradient of the other components in the membrane matrix, according to Equations (28) and (29). Understanding the sorption equilibrium, boundary conditions, and diffusivities is necessary to determine the permeation flow of each component over the polymeric membrane.

Equation (17) can be written in the following form:

$$\ln a_i(\Phi_i, \Phi_j, \Phi_p) = \ln \Phi_i + \frac{z}{2} q_i \ln \left[ \frac{\theta_i}{\Phi_i} \right] + l_i - \sum_{j=1}^n \Phi_j \frac{r_i}{r_j} l_j - r_i \Phi_p \left[ \frac{z}{2} \left[ 1 - \frac{q_p}{r_p} \right] - 1 \right] - q_i^* \ln \sum_{j=1}^n \theta_j^* \tau_{ji} + q_i^* - q_i^* \sum_{j=1}^n \frac{\theta_j^* \tau_{ij}}{\sum_{k=1}^n \theta_k^* \tau_{kj}} \quad (30)$$

The volume fraction ( $\Phi_i, \Phi_j, \Phi_p$ ) are related to each other by the following equation:

$$\Phi_p = 1 - (\Phi_i + \Phi_j) \quad (31)$$

where  $Z$  is the coordination number, which is assumed to be 10,  $q_i$  and  $r_i$  are the molecular surface area and molecular van der Waals volume for pure component  $i$ , and are calculated using the group contribution method [40],  $q_i^*$  is the effective surface of component  $i$ ,  $\Phi_i$  is the volume fraction of component  $i$ ,  $n$  is the number of components,  $\theta_i$  is the surface area fraction of component  $i$ . Lue et.al., [41] reported these data for the toluene-water-PDMS system. The binary interaction parameters  $\tau_{ij}$  and  $\tau_{ji}$  for VOC-water mixtures can be obtained from the vapor-liquid equilibrium data, and the binary interaction parameters between solvent and polymer material ( $\tau_{ip}, \tau_{pi}$  &  $\tau_{jp}, \tau_{pj}$ ) can be obtained from the pure component vapor sorption experiments [42]. The partial derivative of the activity can be represented by differentiating Equation (30) with respect to the component volume fractions  $\Phi_1$  and  $\Phi_2$  as follows:



$$\frac{d \ln a_1}{d \Phi_1} = \frac{1}{\Phi_1} + \frac{z}{2} q_1 \frac{\Phi_1}{\theta_1} \frac{d}{d \Phi_1} \left[ \frac{\theta_1}{\Phi_1} \right] - l_1 + r_1 \left[ \frac{z}{2} \left( 1 - \frac{q_p}{r_p} \right) - 1 \right] - \frac{q_1^*}{\sum_{j=1}^n \theta_j^* \tau_{j1}} \left[ \sum_{j=1}^m \left( \tau_{j1} \frac{d \theta_j^*}{d \Phi_1} \right) \right] - \frac{q_1^* \sum_{j=1}^n \frac{(\sum_{k=1}^m \theta_k^* \tau_{kj}) \left( \frac{d \theta_j^*}{d \Phi_1} \tau_{1j} \right) - (\theta_j^* \tau_{1j}) (\sum_{k=1}^m \tau_{kj} \frac{d \theta_k^*}{d \Phi_1})}{(\sum_{k=1}^m \theta_k^* \tau_{kj})^2}}{(\sum_{k=1}^m \theta_k^* \tau_{kj})^2} \quad (32)$$

$$\frac{d \ln a_1}{d \Phi_2} = \frac{z}{2} q_1 \frac{\Phi_1}{\theta_1} \frac{d}{d \Phi_2} \left[ \frac{\theta_1}{\Phi_1} \right] - \frac{r_1}{r_2} l_2 + r_1 \left[ \frac{z}{2} \left( 1 - \frac{q_p}{r_p} \right) - 1 \right] - \frac{q_1^*}{\sum_{j=1}^n \theta_j^* \tau_{j1}} \left[ \sum_{j=1}^m \left( \tau_{j1} \frac{d \theta_j^*}{d \Phi_2} \right) \right] - \frac{q_1^* \sum_{j=1}^n \frac{(\sum_{k=1}^m \theta_k^* \tau_{kj}) \left( \frac{d \theta_j^*}{d \Phi_1} \tau_{1j} \right) - (\theta_j^* \tau_{1j}) (\sum_{k=1}^m \tau_{kj} \frac{d \theta_k^*}{d \Phi_2})}{(\sum_{k=1}^m \theta_k^* \tau_{kj})^2}}{(\sum_{k=1}^m \theta_k^* \tau_{kj})^2} \quad (33)$$

It is possible to calculate the partial derivatives of Equations (32) and (33) as follows:

$$\frac{d}{d \Phi_k} \left( \frac{\theta_i}{\Phi_i} \right) = \frac{-\left( \frac{q_i}{r_i} \right) \sum_{j=1}^m \left[ \frac{d}{d \Phi_k} \left( \frac{q_j \Phi_j}{r_j} \right) \right]}{\left[ \sum_{j=1}^n \Phi_j \left( \frac{q_j}{r_j} \right) \right]^2}, \text{ for all } i \text{ and } k \quad (34)$$

$$\frac{d \theta_i}{d \Phi_k} = \frac{\left[ \sum_{j=1}^m \Phi_j \left( \frac{q_j}{r_j} \right) \right] \left( \frac{q_i}{r_i} \right) \frac{d \Phi_i}{d \Phi_k} - \left( \frac{q_i \Phi_i}{r_i} \right) \sum_{j=1}^m \left[ \frac{d}{d \Phi_k} \left( \frac{q_j \Phi_j}{r_j} \right) \right]}{\left[ \sum_{j=1}^n \Phi_j \left( \frac{q_j}{r_j} \right) \right]^2}, \text{ for all } i \text{ and } k \quad (35)$$

$$\frac{d \theta_i}{d \Phi_k} = \frac{\left[ \sum_{j=1}^m \Phi_j \left( \frac{q_j^*}{r_j} \right) \right] \left( \frac{q_i^*}{r_i} \right) \frac{d \Phi_i}{d \Phi_k} - \left( \frac{q_i^* \Phi_i}{r_i} \right) \sum_{j=1}^m \left[ \frac{d}{d \Phi_k} \left( \frac{q_j^* \Phi_j}{r_j} \right) \right]}{\left[ \sum_{j=1}^n \Phi_j \left( \frac{q_j^*}{r_j} \right) \right]^2}, \text{ for all } i \text{ and } k \quad (36)$$

Presuming the existence of thermodynamic phase equilibrium at the interfaces of both the feed and permeate with the membrane implies an equilibrium in chemical potential represented by the activity of each constituent in the feed and the membrane at their respective interfaces. Correspondingly, the activity of each permeating element matches that within the membrane at the permeate-membrane interface. Hence, the ensuing mathematical expression can be employed to ascertain the volume fraction of components present on both sides of the membrane [43].

$$a_{if} = a_{imf}, \text{ for all } i \quad (37)$$

$$a_{ip} = a_{imp}, \text{ for all } i \quad (38)$$

The variable  $a_{if}$  denotes the activity of component  $i$  within the feed mixture and can be determined by utilizing the UNIQUAC theory for analyzing multi-component liquid mixtures. Meanwhile,  $a_{imf}$  stands for the activity of component  $i$  at the membrane surface on the feed side,  $a_{ip}$  signifies the activity of component  $i$  on the permeate side, derived by dividing the partial pressure of component  $i$  within the permeate by the vapor pressure at a specific temperature, and  $a_{imp}$  represents the activity of component  $i$  at the membrane surface on the permeate side. The computation of volume fractions for components within the membrane on both the feed side and the permeate side involves substituting the activity of component  $i$  within the membrane phase into Equation (30) and subsequently solving the resulting set of non-linear algebraic equations utilizing the MATLAB solve function.

The following assumptions were used in the mathematic model:

- 1) No interspecies interaction in the membrane.
- 2) The membrane's temperature is constant.
- 3) The pressure is equal to the feed side pressure and remains constant across the membrane.
- 4) A thermodynamic equilibrium exists on the membrane surface that is in touch with the feed and permeate sides.
- 5) The system is stable, and components only penetrate one dimensionally through the flat-sheet membrane's thickness.
- 6) The resistance to penetrant transport on the feed-side boundary layer and the microporous support layer is negligible.



### 3. Experimental

#### 3.1 Materials

A commercial hydrophobic membrane (PDMS™ 4060) was supplied by DeltaMem AG, Switzerland. This membrane consists of three layers where the main material is PDMS with cross-link material. The first is a dense active layer supported on an asymmetric porous polyacrylonitrile (PAN) membrane, which acts as a support layer. The third layer is a non-woven polyester fabric that is a support layer. The three layers are collected together to produce PDMS™ 4060. Benzene (99.5% purity) was purchased from Riedel-Dehaenag Seelze-Hannover, Germany. The toluene (99.5% purity) was purchased from Lab-scan. LTD, Dublin, Ireland. Titanium dioxide, an odorless white nanoparticle, was supplied by Hongwa International Group Ltd. China. Distilled water was used to prepare all aqueous solutions.

#### 3.2 Pervaporation process experiments

The experimental arrangement employed for evaluating the pervaporation process was previously detailed in our earlier publication [44]. To summarize, an initial feed solution of 1.5L comprised a toluene-water mixture. A thermal digital water bath (DK-8AXX, MEDITECH, Taichung, China) regulated the feed temperature within the range of 303 to 323K. A diaphragm pump (BD, 400GPD, Waterpal International Co., Ltd., Kaohsiung City, Taiwan) facilitated the conveyance of the feed mixture to the membrane cell.

The toluene concentration in the feed spanned from 100 to 500 ppm, whereas concentrations varied from 100 to 1000 ppm for the benzene-water blend. The feed flow rate ranged between 1.5 to 3.5 L/min. An effective area of 26.5 cm<sup>2</sup> supported the PDMS membrane, situated atop a perforated plate. A single-stage vacuum pump (B-42, Sigma, Shanghai, China) sustained a downstream vacuum pressure of 2.0 kPa within the module. The collection of permeate samples transpired within a vapor trap immersed in liquid nitrogen. Measurement of the toluene and water content in the permeate occurred using a UV-visible spectrophotometer (V-630, Jasco, with a maximum wavelength at 260 nm, Tokyo, Japan), while a computerized balance (SARTORIUS AC, Goettingen, Germany) with a precision of 0.001 g facilitated permeate weight determination.

### 4. Results and discussion

The parameters governing the interaction between volatile organic compounds (VOCs) and water can be derived from vapor-liquid equilibrium (VLE) data, while the activity of components is computed employing Equation (11). Utilizing the flux values obtained from pervaporation (PV) experiments in conjunction with the proposed model for hydrophobic polymeric membranes, the diffusivities of the constituents are determined. Figures 3 to 6 depict the correlation between diffusivity and VOC activity at various temperatures for both VOC and water. Notably, an increase in VOC activity corresponded to an elevation in VOC diffusivity across the PDMS membrane, suggesting a plausible impact of plasticization. This effect arises from the expansion of free volume amid polymeric chains, facilitating enhanced molecule diffusion through the membrane matrix (as observed in Figure 3 and Figure 5).

Conversely, the relationship between water diffusivity and VOC activity at different temperatures showcased a decrease across the PDMS membrane with escalating VOC activity (as observed in Figure 4 and Figure 6). This phenomenon is attributed to water molecules clustering due to hydrogen bonding, subsequently diminishing their diffusivity and permeability.

The relationship of diffusivity through PDMS membranes for benzene-water systems can be stated as follows:

$$D_B = 1 \times 10^{-10} e^{\beta_B a_{B,f}} \quad (39)$$

$$D_w = 8.666 \times 10^{-8} e^{\beta_w a_{B,f}} \quad (40)$$

where  $D_B$  and  $D_w$  are the diffusivity of benzene and water, respectively,  $a_{B,f}$  is the activity of benzene in feed, and  $\beta_B$  and  $\beta_w$  are the plasticization parameters for benzene and water respectively, which depend on the temperature and the benzene concentration and were calculated and presented in Table (1).

**Table 1:** The values of parameters to estimate plasticization parameter for the benzene-water system

Benzene-Water system	A1	A2	A3	A4
$\beta_B=(A1 \times \log(x_1)-A2) \times T+(A3 \times \log(x_1)+A4)$	-0.221	1.7426	68.57	548.9
$\beta_w=(A1 \times \log(x_1)-A2) \times T+(A3 \times \log(x_1)+A4)$	-0.345	2.9007	106.01	882.24

The parameters A1, A2, A3, and A4 correspond to the benzene and water constituents. They can be determined by adjusting the diffusivity within Equations (39 and 40) to align with the empirical values extracted from the data points of diffusivity coefficients. Meanwhile,  $x_1$  denotes the mole fraction of benzene present in the feed. Similarly, a statement regarding the diffusivity relationship across PDMS membranes for the toluene-water system can be articulated as follows:

$$D_T = 6.666 \times 10^{-10} e^{\beta_T a_{T,f}} \quad (41)$$

$$D_w = 2 \times 10^{-7} e^{\beta_w a_{T,f}} \quad (42)$$

where  $D_T$  and  $D_w$  are the diffusivity of toluene and water, respectively,  $a_{T,f}$  is the activity of toluene in feed, and  $\beta_T$  and  $\beta_w$  are the plasticization parameters for toluene and water, respectively. All toluene-water system data were calculated and presented in Table (2).

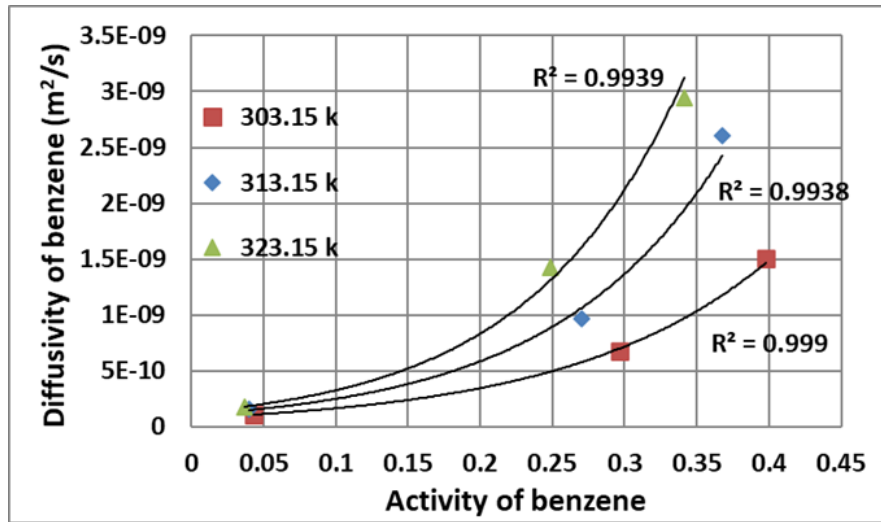


Figure 3: Diffusivity of benzene through PDMS membrane versus activity of benzene at different temperatures

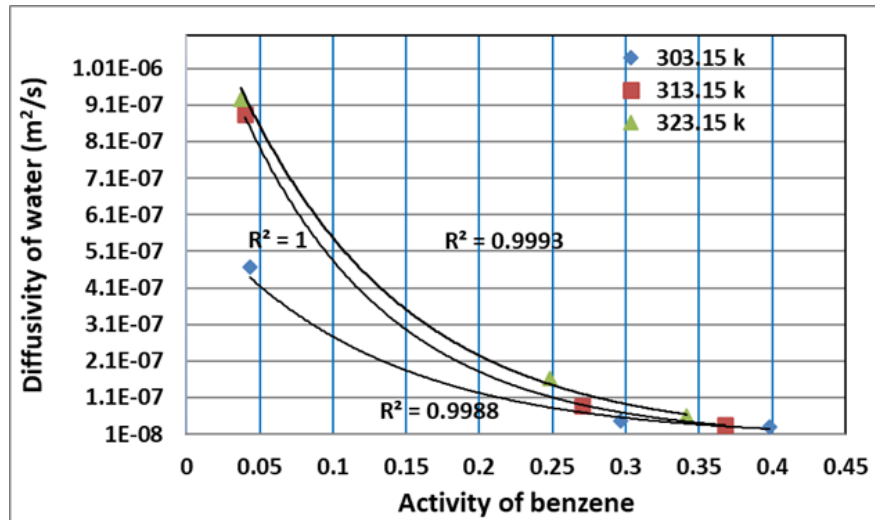


Figure 4: Diffusivity of water through PDMS membrane versus activity of benzene at different temperatures

Table 2: The values of parameters to estimate plasticization parameter for the toluene-water system

Toluene-Water system	A1	A2	A3	A4
$\beta_T = ((A1 \times x_1 + A2) \times T) + (A3 \times x_1 - A4)$	-2055.1	0.2278	646047	69.724
$\beta_w = (A1 \times \log(x_1) - A2) \times T + (A3 \times \log(x_1) + A4)$	-0.156	1.4278	49.346	449.21

The parameters A1, A2, A3, and A4 pertain to the toluene and water constituents, and their determination involves adjusting the diffusivity within Equations (41 and 42) to align with the empirical values derived from the data points of diffusivity coefficients. Concurrently,  $x_1$  represents the mole fraction of toluene in the feed solution.

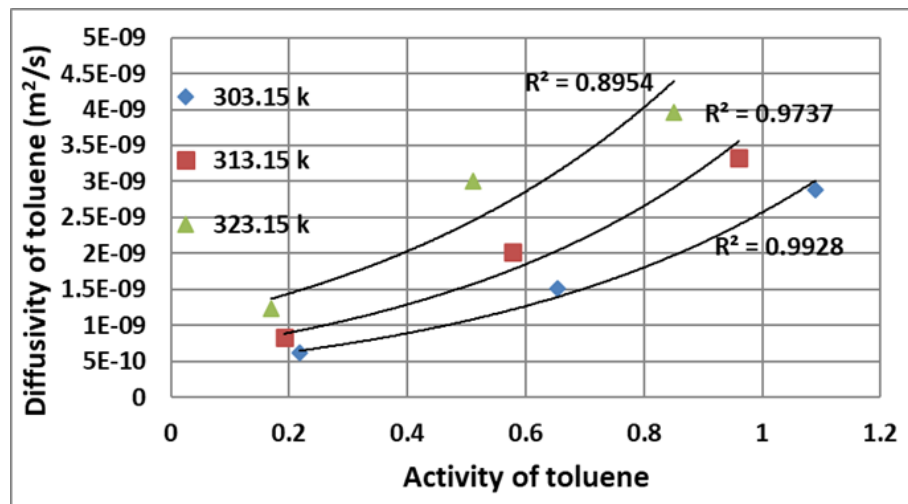


Figure 5: Diffusivity of toluene through PDMS membrane versus activity of toluene at different temperatures

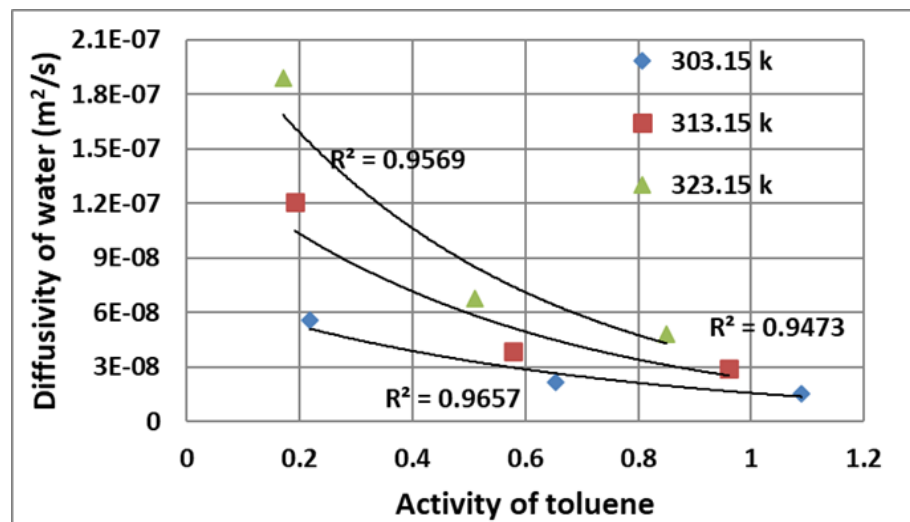


Figure 6: Diffusivity of water through PDMS membrane versus activity of toluene at different temperatures

#### 4.1 Effect of the temperature on permeate flux

The experimental outcomes portraying the benzene-water permeation flux across the PV membrane under varying temperatures are depicted in Figures (7a and b). For an initial benzene concentration of 500 ppm, the benzene flux through the membrane escalated from 88 to 185 g/m<sup>2</sup>·h, accompanied by a concurrent rise in water flux from 342 to 1030 g/m<sup>2</sup>·h. Likewise, Figures (8a and b) delineate the influence of toluene-water feed temperature on the permeation flux of toluene and water, maintaining a toluene feed concentration of 300 ppm. Notably, the toluene flux increased from 55 to 100.75 g/m<sup>2</sup>·h, while the water flux rose from 313 to 850 g/m<sup>2</sup>·h. The depicted graphs show a direct correlation between the rise in permeate flux and elevated temperature. This phenomenon can be attributed to the expanded separation between polymer chains at higher temperatures, consequently augmenting the available free volume for molecular transport [45]. Moreover, the escalation in temperature coincided with an increase in the vapor pressure of each compound, intensifying the driving force across the membrane. Consequently, this led to a notable surge in penetration flux for all compounds [46].

Simultaneously, an observation drawn from both figures highlights the proposed model's robust predictive capability in delineating the impact of feed temperature on the partial fluxes. Notably, the congruence between the predicted and measured values indicates a commendable alignment.

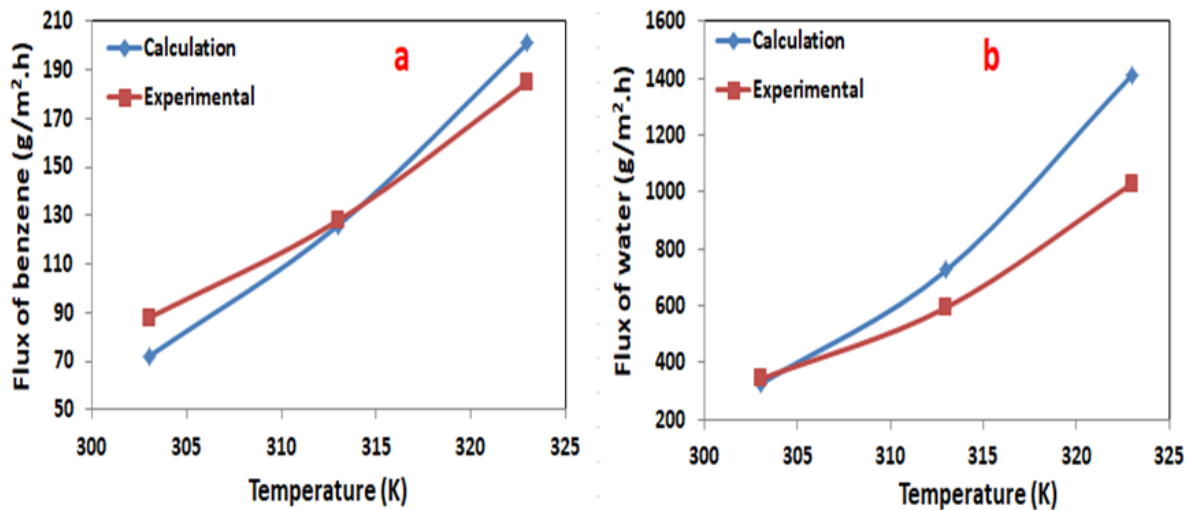


Figure 7: Effect of temperature at an initial benzene feed concentration of 500 ppm on the fluxes of (a) benzene experimental and predicted (b) water experimental and predicted

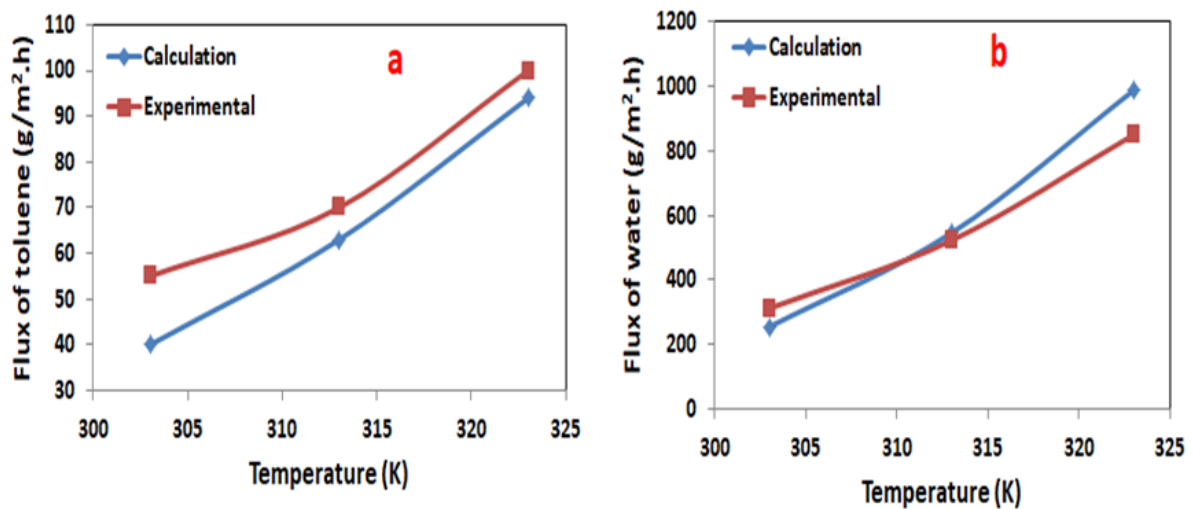


Figure 8: Effect of temperature at an initial toluene feed concentration of 300 ppm on the fluxes of (a) toluene experimental and predicted (b) water experimental and predicted

#### 4.2 Effect of feed concentration on permeation flux

The investigation delved into experimentally examining the impact of varying VOCs feed concentrations on the permeation attributes of the membrane, subsequently comparing the results with the anticipated data presented in Figures (9a and b). Both the experimental and predicted outcomes revealed a consistent trend: an escalation in the feed concentration corresponded to an increase in the flux of the benzene compound. Specifically, the experimental flux elevated from 20 to 165 g/m<sup>2</sup>.h, whereas the predicted flux ranged from 18 to 190 g/m<sup>2</sup>.h, as depicted in Figures (9a). Interestingly, alterations in benzene concentration within the feed solution induced shifts in the water flux behavior. In particular, the water flux declined from 578 to 246 g/m<sup>2</sup>.h for the experimental results and from 630 to 215 g/m<sup>2</sup>.h for the predicted results, illustrated in Figures (9b).

Simultaneously, the experimental and predicted data for toluene flux demonstrated an upward trend, escalating from 17 to 147 g/m<sup>2</sup>.h and 16 to 113 g/m<sup>2</sup>.h, respectively, as depicted in Figures (10a). In contrast, water fluxes declined, decreasing from 353 to 180 g/m<sup>2</sup>.h in the experimental results and from 357 to 247 g/m<sup>2</sup>.h in the predicted results, as illustrated in Figure (10b).

The depicted figures distinctly indicate that augmenting the concentration of VOCs in the feed results in an amplified driving force between the upstream and downstream sections across the membrane. Moreover, this outcome can be elucidated by the phenomenon wherein water molecules tend to cluster due to hydrogen bonding interactions, subsequently diminishing their diffusivity and permeability [47].

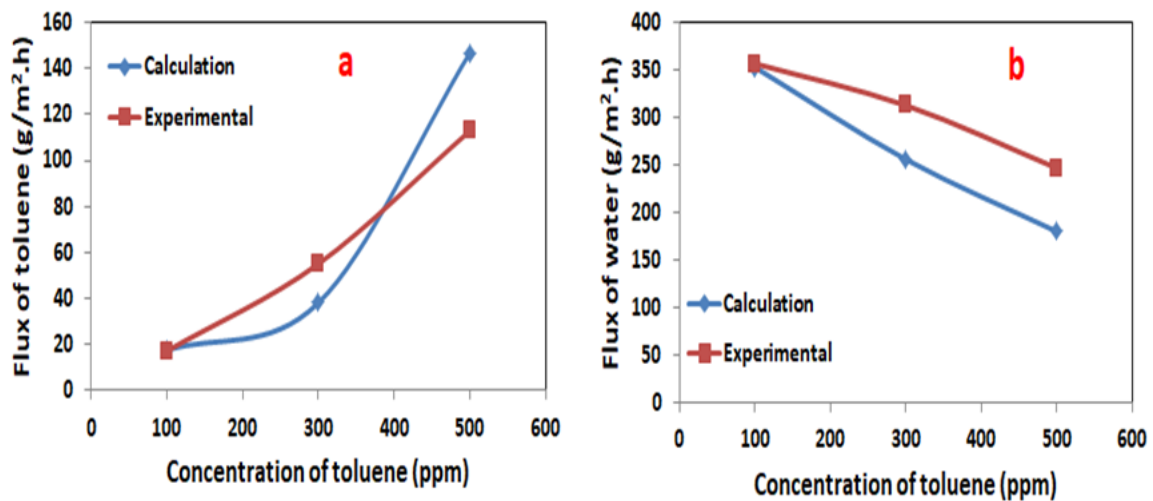


Figure 9: Effect of the benzene feed concentration at feed temperature of 303K on fluxes of (a) benzene experimental and predicted (b) water experimental and predicted

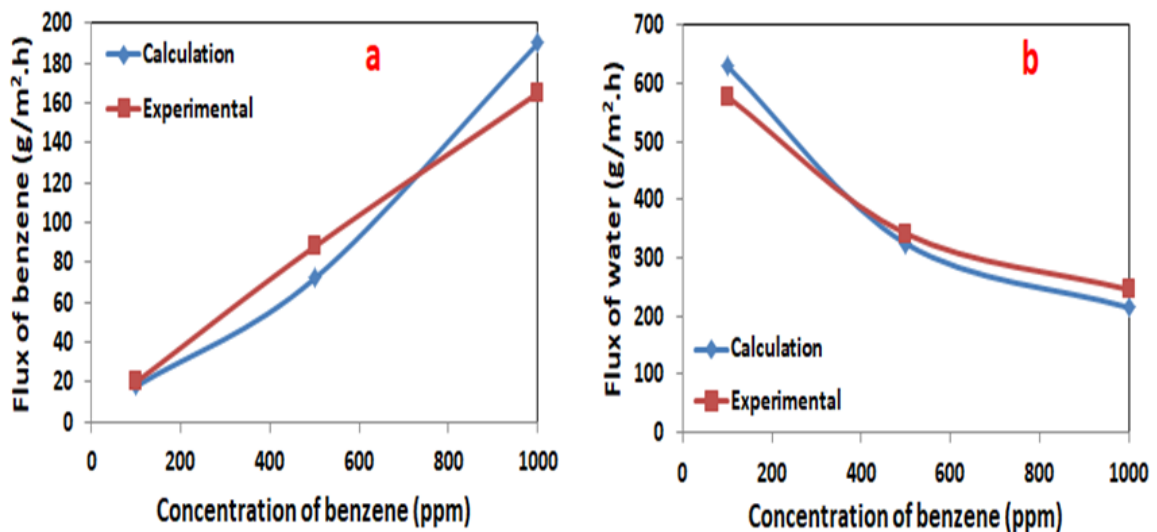


Figure 10: Effect of the toluene feed concentration at feed temperature of 303K on fluxes of (a) toluene experimental and predicted (b) water experimental and predicted

The experimental and modeled fluxes were juxtaposed for benzene and water in a benzene-water system and for toluene and water in a toluene-water system, as depicted in Figures (11a), (11b), (12a) and (12b).

At lower feed concentrations, the predictions generated by the proposed mathematical model, aimed at elucidating partial flux permeation for benzene, toluene, and water, exhibited a noteworthy concurrence with the acquired experimental data. However, it's evident that with increasing VOC concentrations, a proportional rise in inaccuracies within the predictions was observed. These discrepancies may be attributed to the failure of the experiment to attain the presumed activity equality between the feed and the membrane surface. Consequently, at high VOC concentrations, the model's precision in computing the volume fraction of components at the membrane surface becomes compromised. Notably, achieving activity equilibrium is more feasible at lower VOC concentrations, allowing for characteristic agreement between predicted and experimental data. Contrastingly, the prevalent non-equilibrium intensifies at higher concentrations, exacerbating computational errors. Additionally, the proposed model does not incorporate concentration polarization in the pervaporation membrane process, potentially leading to considerable deviations.

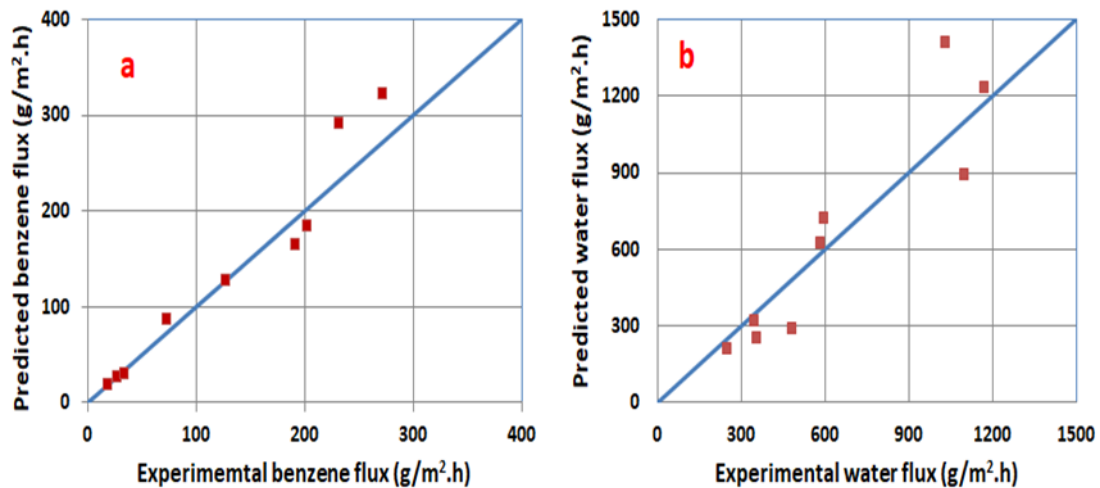


Figure 11: Comparison of predicted and experimental permeation fluxes of (a) benzene (g/m<sup>2</sup>.h) and (b) water (g/m<sup>2</sup>.h) in the benzene-water system

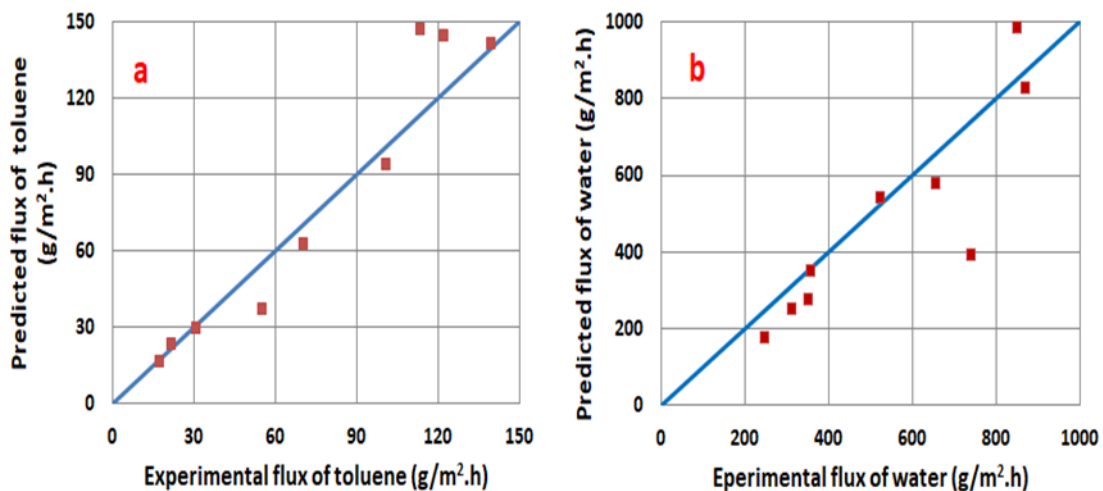


Figure 12: Comparison of predicted and experimental permeation fluxes of (a) toluene (g/m<sup>2</sup>.h) and (b) water (g/m<sup>2</sup>.h) in the toluene-water system

## 5. Conclusion

An experimental approach and a mathematical model were employed to assess the permeability of the commercial PV-PDMS<sup>TM</sup>4060 membrane when exposed to VOCs feed solutions, considering various feed temperatures and initial concentrations of benzene and toluene. Leveraging the solution-diffusion model, a framework was devised to estimate the permeation flux in the pervaporation (PV) process to extract benzene and toluene from aqueous solutions via the membrane. Findings indicated that the VOCs' flux heightened alongside elevated feed temperatures and initial concentrations of benzene and toluene in the feed solution. Moreover, the solution-diffusion model aptly represented the permeation flow within a dense membrane. This model crucially incorporates two phases—sorption and diffusion of constituents across the membrane—to compute mass transfer rates. An amalgamated model was proposed, merging the fundamental transport equation of the solution-diffusion theory with the UNIQUAC model. Remarkably, it was revealed that the diffusivity of VOCs across the membrane exhibited an exponential increase corresponding to augmented feed VOCs activity, whereas water diffusivity witnessed a decrease. Notably, the proposed model accurately predicted the influence of feed concentration and temperature on partial fluxes, showcasing acceptable agreement between predicted and measured values.

### Author contributions

Conceptualization, Q. Alsahy and S. Rasheed.; methodology, S. Ibrahim.; software, S. Rasheed.; validation, A. Abbas., R. Al-Jaboory and Z. Jawad.; formal analysis, L. Chun.; investigation, Q. Alsahy.; resources, S. Ibrahim.; data curation, S. Rasheed.; writing—original draft preparation, S. Rasheed.; writing—review and editing, Q. Alsahy.; visualization, S. Rasheed.;



supervision, S. Ibrahim.; project administration, Q. Alsally. All authors have read and agreed to the published version of the manuscript.

### Funding

This research received no specific grant from any funding agency in the public, commercial, or not-for-profit sectors.

### Data availability statement

The data that support the findings of this study are available on request from the corresponding author.

### Conflicts of interest

The authors declare that there is no conflict of interest.

### References

- [1] S. H. Rasheed, S. S. Ibrahim, Q. F. Alsally, and H. Sh. Majdi, Polydimethylsiloxane (PDMS) Membrane for Separation of Soluble Toluene by Pervaporation Process, *Membr. J.*, 13 (2023) 289. <https://doi.org/10.3390/membranes13030289>
- [2] T.K. Abbas, K.T. Rashid, S. Al-Saady, A.A. Alsarayreh, A. Figoli, Q.F. Alsally, Decontamination of Aqueous Nuclear Waste via Pressure-driven Membrane Application—A Short Review, *Eng. Technol. J.*, 41 (2023) 1152- 1174. <https://doi.org/10.30684/etj.2023.140193.1454>
- [3] S. Shukla, J. Méricq, M. Belleville, N. Hengl, N. Benes, I. Vankelecom, J.S. Marcano, Process intensification by coupling the Joule effect with pervaporation and sweeping gas membrane distillation, *J. Membr. Sci.*, 545 (2018) 150-157. <https://doi.org/10.1016/j.memsci.2017.09.061>
- [4] M. Rezakazemi, M. Sadrzadeh, T. Mohammadi, Separation via pervaporation techniques through polymeric membranes, Transport properties of polymeric membranes, Elsevier Amsterdam, 2018, pp. 243-263. <http://dx.doi.org/10.1016/B978-0-12-809884-4.00013-6>
- [5] D.L. Oatley-Radcliffe, S. Al-Aani, P.M. Williams, N. Hilal, Chapter 15 - Mass Transport in Porous Liquid Phase Membranes, in: N. Hilal, A.F. Ismail, T. Matsuura, D. Oatley-Radcliffe (Eds.), *Membrane Characterization*, Elsevier 2017, pp. 337-358. <https://doi.org/10.1016/B978-0-444-63776-5.00015-2>.
- [6] L.M. Vane, F.R. Alvarez, Vibrating pervaporation modules: Effect of module design on performance, *J. Membr. Sci.*, 255 (2005) 213-224. <https://doi.org/10.1016/j.memsci.2005.01.047>
- [7] F. Lipnizki, G. Trägårdh, Modelling of pervaporation: Models to analyze and predict the mass transport in pervaporation, *Sep. Purif. Methods*, 30 (2001) 49-125. <https://doi.org/10.1081/SPM-100102985>
- [8] D.S. Abrams, J.M. Prausnitz, Statistical thermodynamics of liquid mixtures: a new expression for the excess Gibbs energy of partly or completely miscible systems, *AIChE J.* 21 (1975) 116-128. <https://doi.org/10.1002/aic.690210115>
- [9] G. Wilson, C. Deal, Activity coefficients and molecular structure. Activity coefficients in changing environments-solutions of groups, *Ind. Eng. Chem. Fundam.*, 1 (1962) 20-23. <https://doi.org/10.1021/i160001a003>
- [10] A. Fredenslund, R.L. Jones, J.M. Prausnitz, Group-contribution estimation of activity coefficients in nonideal liquid mixtures, *AIChE J.*, 21 (1975) 1086-1099. <https://doi.org/10.1002/aic.690210607>
- [11] T. Oishi, J.M. Prausnitz, Estimation of solvent activities in polymer solutions using a group-contribution method, *Ind. Eng. Chem. Process Des. Dev.*, 17 (1978) 333-339. <https://doi.org/10.1021/i260067a021>
- [12] R. Goydan, R.C. Reid, H.S. Tseng, Estimation of the solubilities of organic compounds in polymers by group-contribution methods, *Ind. Eng. Chem. Res.*, 28 (1989) 445-454. <https://doi.org/10.1021/ie00088a012>
- [13] A. Heintz, W. Stephan, A generalized solution—diffusion model of the pervaporation process through composite membranes Part II. Concentration polarization, coupled diffusion and the influence of the porous support layer, *J. Membr. Sci.*, 89 (1994) 153-169. [https://doi.org/10.1016/0376-7388\(93\)E0223-7](https://doi.org/10.1016/0376-7388(93)E0223-7)
- [14] W. Stephan, A. Heintz, Separation of Aliphatic/Aromatic Mixtures by Pervaporation Using Polyurethane Membranes: Model Calculations and Comparison with Experimental Results, Sixth International Conference on Pervaporation Process in the Chemical Industry, 1992.
- [15] S. Ghoreyshi, F. Farhadpour, M. Soltanieh, Multi-component transport across non-porous polymeric membranes, *Desalin.*, 144 (2002) 93-101. [https://doi.org/10.1016/S0011-9164\(02\)00295-3](https://doi.org/10.1016/S0011-9164(02)00295-3)
- [16] Q. Wang, N. Li, B. Bolto, M. Hoang, Z. Xie, Desalination by pervaporation: A review, *Desalination*, 387 (2016) 46-60. <https://doi.org/10.1016/j.desal.2016.02.036>
- [17] S.P. Nunes, K.-V., Peinemann, *Membrane technology*, Wiley Online Library 2001.



- [18] S. Sourirajan, S. Bao, T. Matsuura, An approach to membrane separation by pervaporation, Proceedings of the Second International Conference on Pervaporation Processes in Chemical Industry, San Antonio, TX, USA, 1987, pp. 8-11.
- [19] T. Okada, M. Yoshikawa, T. Matsuura, A study on the pervaporation of ethanol/water mixtures on the basis of pore flow model, *J. Membr. Sci.*, 59 (1991) 151-168. [https://doi.org/10.1016/S0376-7388\(00\)81180-1](https://doi.org/10.1016/S0376-7388(00)81180-1)
- [20] T. Okada, T. Matsuura, A new transport model for pervaporation, *J. Membr. Sci.*, 59 (1991) 133-149. [https://doi.org/10.1016/S0376-7388\(00\)81179-5](https://doi.org/10.1016/S0376-7388(00)81179-5)
- [21] P. Peng, Y. Lan, J. Luo, Modified silica incorporating into PDMS polymeric membranes for bioethanol selection, *Adv. Polym. Technol.*, (2019). <https://doi.org/10.1155/2019/5610282>
- [22] Y. Wang, X. Mei, T. Ma, C. Xue, M. Wu, M. Ji, Y. Li, Green recovery of hazardous acetonitrile from high-salt chemical wastewater by pervaporation, *J. Clean. Prod.*, 197 (2018) 742-749. <https://doi.org/10.1016/j.jclepro.2018.06.239>
- [23] L. Li, Development of pervaporation composite membranes for brine desalination application, Ph.D. Thesis, University of UNSW Sydney, 2018.
- [24] E. Halakoo, Thin film composite membranes via layer-by-layer assembly for pervaporation separation, Ph.D. Thesis, University of Waterloo (2019).
- [25] M.N. Hyder, Preparation, characterization and performance of Poly (vinyl alcohol) based membranes for pervaporation dehydration of alcohols, Ph.D. Thesis, University of Waterloo (2008).
- [26] Q. XIANGYI, The development of pervaporation membranes for alcohol dehydration, Ph.D. Thesis, University of Singapore (2007).
- [27] J.G. Wijmans, R.W. Baker, The solution-diffusion model: a review, *J. Membr. Sci.*, 107 (1995) 1-21. [https://doi.org/10.1016/0376-7388\(95\)00102-1](https://doi.org/10.1016/0376-7388(95)00102-1)
- [28] R. Binning, R. Lee, J. Jennings, E. Martin, Separation of liquid mixtures by permeation, *Ind. Eng. Chem.*, 53 (1961) 45-50.
- [29] R. Binning, F. James, Permeation. A new commercial separation tool, *Petroleum Refiner.*, 39 (1958) 88.
- [30] T. Graham, LV. On the absorption and dialytic separation of gases by colloid septa, *Lond. Edinb. Dublin philos. Mag. J. Sci.*, 32 (2009) 401-420. <https://doi.org/10.1080/14786446608644207>
- [31] J.-J. Shieh, R.Y. Huang, A pseudophase-change solution-diffusion model for pervaporation. I. Single component permeation, *Sep. Sci. Technol.*, 33 (2008) 767-785. <http://dx.doi.org/10.1080/01496399808544875>
- [32] J.-J. Shieh, R.Y. Huang, A pseudophase-change solution-diffusion model for pervaporation. II. Binary mixture permeation, *Sep. Sci. Technol.*, 33 (1998) 933-957.
- [33] R.W. Baker, Membrane technology and applications, John Wiley & Sons, UK, 2023.
- [34] F. Lipnizki, S. Hausmanns, P.-K. Ten, R.W. Field, G. Laufenberg, Organophilic pervaporation: prospects and performance, *Chem. Eng. J.*, 73 (1999) 113-129. [https://doi.org/10.1016/S1385-8947\(99\)00024-8](https://doi.org/10.1016/S1385-8947(99)00024-8)
- [35] S.C. George, S. Thomas, Transport phenomena through polymeric systems, *Prog. Polym. Sci.*, 26 (2001) 985-1017. [https://doi.org/10.1016/S0079-6700\(00\)00036-8](https://doi.org/10.1016/S0079-6700(00)00036-8)
- [36] M. Mulder, Preparation techniques for immersion precipitation, *Basic Principles of Membrane Technology*. Kluwer Academic Publishers, Dordrecht (1996) 77-81.
- [37] Q.N. Trong, Modelling of the influence of downstream pressure for highly selective pervaporation, *J. Membr. Sci.*, 34 (1987) 165-183. [https://doi.org/10.1016/S0376-7388\(00\)80030-7](https://doi.org/10.1016/S0376-7388(00)80030-7)
- [38] S.N. Kim, K. Kammermeyer, Actual concentration profiles in membrane permeation, *Sep. Sci.*, 5 (1970) 679-697. <https://doi.org/10.1080/00372367008055530>
- [39] R. Kamesh, S. Chenna, K.Y. Rani, Thermodynamic models for prediction of sorption behavior in pervaporation, *Membrane Processes: Pervaporation, Vapor Permeation and Membrane Distillation for Industrial Scale Separations* (2018) 169-209. <https://doi.org/10.1002/9781119418399.ch6>
- [40] R. Kamesh, S. Chenna, K.Y. Rani, Thermodynamic Models for Prediction of Sorption Behavior in Pervaporation, *Membr. Process.*, (2018) 169-209. <http://dx.doi.org/10.1002/9781119418399.ch6>
- [41] S. J. Lue, S.Y. Wu, S.F. Wang, L.D. Wang, C.L. Tsai, Modeling multi-component vapor sorption in a poly(dimethyl siloxane) membrane, *Desalination*, 233 (2008) 286-294. <https://doi.org/10.1016/j.desal.2007.09.053>
- [42] J. Hauser, A. Heintz, B. Schmittecker, R.N. Lichtenthaler, Sorption equilibria and diffusion in polymeric membranes, *Fluid Ph. Equilibria.*, 51 (1989) 369-381. [https://doi.org/10.1016/0378-3812\(89\)80377-2](https://doi.org/10.1016/0378-3812(89)80377-2)

- [43] S.H. Rasheed, S.S. Ibrahima, A. Zrellib, A. Figolic, A. Alhathal, Q.F.A. AlAnezid, A Review on the Separation of Volatile Organic Compounds from Wastewater by Pervaporation Processes, *Eng. Technol. J.*, 41 (2023) 512-528. <https://doi.org/10.30684/etj.2023.138340.1386>
- [44] S.H. Rasheed, S.S. Ibrahim, Q.F. Alsahy, H.S. Majdi, Polydimethylsiloxane (PDMS) Membrane for Separation of Soluble Toluene by Pervaporation Process, *Membranes*, 13 (2023) 289. <https://doi.org/10.3390/membranes13030289>
- [45] G.O. Yahaya, Separation of volatile organic compounds (BTEX) from aqueous solutions by a composite organophilic hollow fiber membrane-based pervaporation process, *J. Membr. Sci.*, 319 (2008) 82-90. <https://doi.org/10.1016/j.memsci.2008.03.024>.
- [46] M. Aliabadi, A. Aroujalian, A. Raisi, Removal of styrene from petrochemical wastewater using pervaporation process, *Desalination*, 284 (2012) 116-121. <https://doi.org/10.1016/j.desal.2011.08.044>.
- [47] L.Y. Ng, A.W. Mohammad, C.P. Leo, N. Hilal, Polymeric membranes incorporated with metal/metal oxide nanoparticles: A comprehensive review, *Desalination*, 308 (2013) 15-33. <https://doi.org/10.1016/j.desal.2010.11.033>.